Bulletin of Electrical Engineering and Informatics
Vol. 11, No. 2, April 2022, pp. 838∼845
ISSN: 2302-9285, DOI: 10.11591/eei.v11i2.3138

Ergodic capacity of internet of things' devices in presence of channel state information imperfection

Dinh-Thuan Do, Anh-Tu Le
Faculty of Electronics Technology, Industrial University of Ho Chi Minh City, Ho Chi Minh City, Vietnam

Article Info

Article history:

Received Jul 14, 2021
Revised Dec 27, 2021
Accepted Feb 24, 2022

Keywords:

Channel state information
Ergodic capacity
Internet of things

ABSTRACT

Non-orthogonal multiple access (NOMA) is deployed to improve spectral efficiency for applications in fifth generation networks. NOMA system splits power domain to many parts to further serve massive users by relaxing the orthogonal use of radio-resources. In this paper, a relay is required to help the source communicate with destinations with a fixed power allocation scheme. We derive expressions to highlight ergodic performance of two users the deployment of NOMA is suitable to different rate requirements from destinations (e.g., a cellular users have different requirements compared with internet of things devices). By conducting Monte-Carlo simulations, we find main system parameters which have crucial impacts on ergodic capacity. This paper is different other recent studies since we emphasize on imperfect channel state information (CSI) and Rician fading model for our analytical results.

Corresponding Author:

Anh-Tu Le
Faculty of Electronics Technology, Industrial University of Ho Chi Minh City
12 Nguyen Van Bao, Ho Chi Minh City 700000, Vietnam
Email: leanhtu@iuh.edu.vn

1. INTRODUCTION

In recent years, power-domain based non-orthogonal multiple access (NOMA) has recently studied as a promising system to enhance system performance in terms of low latency, high efficiency, and massive users [1]-[3]. Since only a fraction of total transmit power is assigned to NOMA user is allocated, the limited coverage of NOMA-based system is raised compared with the traditional (OMA)-based system. As one of the effective methods is to improve the coverage, once might integrate the cooperative approaches into NOMA systems. To assist the transmission between the transmitter and NOMA users, such system needs assistance from a certain number of intermediate nodes. By owing to the spatial diversity gain, NOMA relaying systems have benefits of the reception reliability [4]. The two kinds of cooperative NOMA networks are the dedicated-relay cooperation and the user cooperation, which depends on the role of relay. In the dedicated-relay cooperation, relays are required to forward signal from the source to destinations [5]-[12]. In the user cooperation, relays are strong users which help foster communication from the source to weak users [13].

In the perspective of internet of things (IoT) for sixth-generation (6G), the system in [14] needs cover spectrum access for huge number of users relying on allowed spectrum resources. In traditional systems, the overuse of spectrum resources related to access of orthogonal multiple signal is challenging [14] proposed 6G-enabled cognitive IoT (CIoT) by exploiting a NOMA-adied hybrid spectrum access approach. In this scenario, both the busy and idle spectrum are accessed by the CIoT without considering the primary users' state. The work in [15] studied system to serve massive IoT devices in extremely differentiated IoT applications for 6G. Such system is able to provide communication in air-space-ground integrated system. To support IoT

deployment in remote and disaster areas, by deploying unmanned aerial vehicle (UAV), such UAV can act as aerial base station to communicate with users in cluster of UAV-supported clustered users. In addition, an aerial base station along with wireless powered communication (WPC)-based UAV provides higher energy efficiency.

Different from aforementioned conventional NOMA systems, half-duplex and relay stations (RSs) schemes benefit to NOMA approach since they exhibit further gains in term of spatial diversity [16]–[23]. Yue *et al*. in [18], Kader *et al*. [20], and Liang *et al*. [21], the transmission from transmitters to receivers needs assistance of a single relay. Main results in [18], [21] indicated that the orthogonal multiple access (OMA) is likely worse than the system relying on NOMA when we mentioned system performance metrics including throughput and outage probability. The popular models of channels namely Nakagami-m fading channels [18] and Rayleigh fading channels [21] are considered as best fit to characterize advances of NOMA systems. Kader *et al*. in [20], ergodic sum capacity with perfect and imperfect successive interference cancellation (SIC) are analysed to highlight performance of the cooperative NOMA relaying system including two transmitters, a single shared relay and two destinations. However, there is still open problem regarding how we can achieve exact channel information at receivers. Motivated by recent work [20], this paper focuses on the impact of imperfect channel state information (CSI) in downlink dual-hop NOMA system. Importantly, we characterize channels as Rician fading model to provide analytical computations of outage probability for destinations.

2. SYSTEM MODEL

We consider a downlink dual-hop NOMA network which consists a base station (S) and two devices $U_i (i\{1; 2\})$, shown in in Figure 1. To extend coverage, the destinations need the help of a relay (R) which operates in a decode-and-forward (DF) mode. We denote the distances from S to R and R to U_i are d_{SR} and d_{RU_i}, respectively. In addition, we denote h_{SR}, h_{RU_i} are the Rician fading channel form S to R and R to U_i respectively [22].

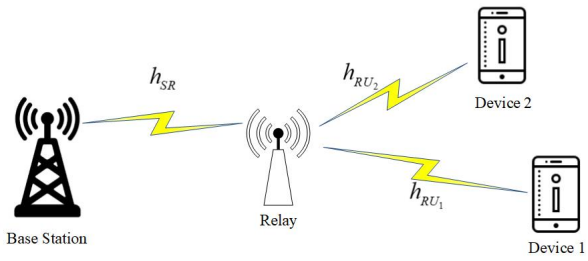

Figure 1. The system model of downlink dual-hop NOMA

This paper emphasizes on the impact of CSI on system performance analysis. In particular, the channel estimation error can be modeled as [23]:

$$h_v = \hat{h}_v + \hbar_v; \tag{1}$$

where $v \in \{SR; RU_1; RU_2\}$, $\hat{h}_v$ is the estimated channel coefficient and $\hbar_v$ is the error term with $CN(0; \sim_v^2)$.

In this first phase, S send superimposed signal to R. The received signal at R is expressed as:

$$\begin{aligned} y_R &= \sqrt{P_S d_{SR}}\,(\sqrt{\ }x_1 + (1-\ )x_2)\ \hat{h}_{SR} + \hbar_{SR}\ + n_{SR} \\ &= \sqrt{P_S d_{SR}}\hat{h}_{SR}\,(\sqrt{\ }x_1 + (1-\ )x_2) \\ &+ \sqrt{P_S d_{SR}}\hbar_{SR}\,(\sqrt{\ }x_1 + (1-\ )x_2) + n_{SR}; \end{aligned} \tag{2}$$

where P_S is the transmit power at S, denotes the path-loss exponent, x_i is the the intended message to U_i, is the power allocation coefficient with $> 0{:}5$, and n_{SR} is the additive white Gaussian noise (AWGN) with $CN(0; N_0)$.

To compute the outage probability, we need to determine the signal-to interference-plus-noise ratio

(SINR) which is used to detect signal x_1 at R, and such SINR is formulated by:

$$\begin{aligned} {}^{x_1}_{R} &= \frac{P_S d_{SR}^{\quad} \left|\hat{h}_{SR}\right|^2}{P_S d_{SR} (1-\ ) \left|\hat{h}_{SR}\right|^2 + P_S d_{SR} \sim_{SR}^2 + N_0} \\ &= \frac{d_{SR}^{\quad} \left|\hat{h}_{SR}\right|^2}{d_{SR} (1-\ ) \left|\hat{h}_{SR}\right|^2 + \ d_{SR} \sim_{SR}^2 + 1}; \end{aligned} \tag{3}$$

where $= \frac{P_S}{N_0}$ is the transmit signal-to-noise ratio (SNR).

By doing SIC to delete interference, the SNR at R is used to detect signal x_2 and it is expressed by:

$${}^{x_2}_{R} = \frac{d_{SR} (1-\ ) \left|\hat{h}_{SR}\right|^2}{d_{SR} \sim_{SR}^2 + 1}: \tag{4}$$

In the second phase, the received signal at U_i when R forwards signal from S to U_i is formulated by:

$$\begin{aligned} y_{RU_i} = & \sqrt{P_R d_{RU_i}} \hat{h}_{RU_i} (\ x_1 + (1-\ ) x_2) \\ & + \sqrt{P_R d_{RU_i}} h_{RU_i} (\ x_1 + (1-\ ) x_2) + n_{RU_i}; \end{aligned} \tag{5}$$

where P_R is the transmit power at R and n_{RU_i} is AWGN with $CN(0; N_0)$.

At user U_1, two steps are conducted. Firstly, U_1 detects the signal x_1 with SINR is given by:

$${}^{x_1}_{RU_1} = \frac{d_{RU_1}^{\quad} \left|\hat{h}_{RU_1}\right|^2}{d_{RU_1} (1-\ ) \left|\hat{h}_{RU_1}\right|^2 + \ d_{RU_1} \sim_1^2 + 1}; \tag{6}$$

where $= \frac{P_R}{N_0}$. Secondly, U_1 decodes the signal x_1 after performing SIC and the SINR is expressed as:

$${}^{x_2}_{RU_2} = \frac{d_{RU_2} (1-\ ) \left|\hat{h}_{RU_2}\right|^2}{d_{RU_2} \sim_2^2 + 1} \tag{7}$$

Similarly, U_2 detects the own signal x_1 and the SINR is given by:

$${}^{x_1}_{RU_2} = \frac{d_{RU_2}^{\quad} \left|\hat{h}_{RU_2}\right|^2}{d_{RU_2} (1-\ ) \left|\hat{h}_{RU_2}\right|^2 + \ d_{RU_2} \sim_2^2 + 1} \tag{8}$$

To further compute ergodic capacity, we will apply result reported in [24], i.e. the probability distribution function (PDF) of $\hat{h}_v$ is given by:

$$f_{\left|\hat{h}_v\right|^2}(z) = \frac{(K_v + 1) e^{\ K}}{v} e^{\ \frac{(1+K)}{v} z} \mathcal{I}_0 @2 \ \sqrt{\frac{K_v (1+K_v) z}{v}} A \tag{9}$$

where K_v is the Rician factor, $_v$ is the average fading power and $\mathcal{I}_0$ denotes the Bessel function of the first kind [25].

3. THE ANALYSIS OF ERGODIC CAPACITY

In this section, we evaluate the closed-form expression of ergodic capacity for users U_i.

3.1. Ergodic capacity of U_2

The ergodic capacity of U_1 can be expressed as [26]:

$$C_{x_1} = \frac{1}{2\ln 2}\int_0^{Z^1} \frac{1 - F_{Z_1}(x)}{1+x}dx; \tag{10}$$

where $Z_1 = \min\left(\frac{x_1}{R}; \frac{x_1}{RU_1}\right)$.

The cumulative distribution function (CDF) of Z_1 is given as:

$$\begin{aligned} F_{Z_1}(x) = 1 - & \sum_{n_{SR}=0}^{\infty}\sum_{a_{SR}=0}^{m_{SR}}\sum_{n_1=0}^{\infty}\sum_{a_1=0}^{m_1} \frac{K_1^{n_1}K_{SR}^{n_{SR}} e^{-K_{SR}-K_1}}{a_1!n_1!a_{SR}!n_{SR}!} \\ & \times \left(a_{SR}\#a_1\right) e^{\frac{x}{\Omega_{SR}(1-\eta)}x} \left(\frac{\#}{\Omega_1(1-\eta)}x\right)^{a_1} \left(\frac{x}{\Omega_{SR}(1-\eta)}\right)^{a_{SR}} \end{aligned} \tag{11}$$

Putting (11) into (10), C_{x_1} can be expressed by:

$$\begin{aligned} C_{x_1} = & \frac{1}{2\ln 2}\sum_{n_{SR}=0}^{\infty}\sum_{n_1=0}^{\infty}\sum_{a_{SR}=0}^{m_{SR}}\sum_{a_1=0}^{m_1} \frac{K_1^{n_1}K_{SR}^{n_{SR}} e^{-K_{SR}-K_1}\left(a_{SR}\#a_1\right)}{a_1!n_1!a_{SR}!n_{SR}!} \\ & \times \int_0^{(Z^{-})} \frac{e^{\frac{+\#}{\Omega_{SR}(1-\eta)}x}}{1+x} \left(\frac{x}{\Omega_{SR}(1-\eta)}\right)^{a_{SR}+a_1} dx \end{aligned} \tag{12}$$

Using the Gaussian-Chebyshev quadrature [27], the close-form of U_1 is given as:

$$\begin{aligned} C_{x_1} = & \frac{\pi}{2I\ln 2}\sum_{n_{SR}=0}^{\infty}\sum_{n_1=0}^{\infty}\sum_{a_{SR}=0}^{m_{SR}}\sum_{a_1=0}^{m_1} \frac{K_1^{n_1}K_{SR}^{n_{SR}} e^{-K_{SR}-K_1}\left(a_{SR}\#a_1\right)}{a_1!n_1!a_{SR}!n_{SR}!} \\ & \times \sum_{c=1}^{I} \sqrt{1-\vartheta_c^2}\frac{e^{\frac{(1+\vartheta_c)(+\#)}{\Omega_{SR}(1-\eta)(1-\vartheta_c)}}}{2(1-\eta)+(1+\vartheta_c)} \left(\frac{(1+\vartheta_c)}{(1-\eta)(1-\vartheta_c)}\right)^{a_{SR}+a_1}; \end{aligned} \tag{13}$$

where $\vartheta_c = \cos\left(\frac{2c-1}{2I}\pi\right)$.

3.2. Ergodic capacity of U_1

Similarly, the ergodic capacity of of U_2 is calculated by:

$$C_{x_2} = \frac{1}{2\ln 2}\int_0^{Z^1} \frac{1 - F_{Z_2}(x)}{1+x}dx; \tag{14}$$

where $Z_2 = \min\left(\frac{x_2}{R}; \frac{x_2}{RU_2}\right)$. Similarly, the CDf of Z_2 is given as:

$$\begin{aligned} F_{Z_2}(x) = 1 - & \sum_{n_{SR}=0}^{\infty}\sum_{a_{SR}=0}^{m_{SR}}\sum_{n_2=0}^{\infty}\sum_{a_2=0}^{m_2} \frac{K_2^{n_2}K_{SR}^{n_{SR}} e^{-K_2}e^{-K_{SR}}}{a_2!n_2!a_{SR}!n_{SR}!} \\ & \times e^{-\left(\frac{+\$}{\Omega_{SR}(1-\eta)}\right)x} \left(\frac{x}{\Omega_{SR}(1-\eta)}\right)^{a_{SR}} \left(\frac{\$x}{\Omega_2(1-\eta)}\right)^{a_1} \end{aligned} \tag{15}$$

Next, C_{x_2} is rewritten as:

$$\begin{aligned} C_{x_2} = & \sum_{n_{SR}=0}^{\infty}\sum_{a_{SR}=0}^{m_{SR}}\sum_{n_2=0}^{\infty}\sum_{a_2=0}^{m_2} \frac{K_2^{n_2}K_{SR}^{n_{SR}} e^{-K_2}e^{-K_{SR}}}{a_2!n_2!a_{SR}!n_{SR}!} \\ & \times \frac{a_{SR}\$^{a_1}}{\Omega_{SR}^{a_{SR}+a_1}(1-\eta)^{a_{SR}+a_1}} \int_0^{Z^1} \frac{x^{a_{SR}+a_1}}{1+x} e^{-\left(\frac{+\$}{\Omega_{SR}(1-\eta)}\right)x}. \end{aligned} \tag{16}$$

Then, we express C_{x_2} as:

$$C_{x_2} = \sum_{n_{SR}=0}^{n_{SR}} \sum_{a_{SR}=0}^{a_{SR}} \sum_{n_2=0}^{n_2} \sum_{a_2=0}^{a_2} \frac{K_2^{n_2} K_{SR}^{n_{SR}} e^{-K_2} e^{-K_{SR}}}{a_2! n_2! a_{SR}! n_{SR}!} \times \frac{a_{SR}\$^{a_1}}{(1-)^{a_{SR}+a_1}} (-1)^{a_{SR}+a_1-1} e^{\frac{+\$}{(1-)}} Ei\left(-\frac{+\$}{1-}\right) + \sum_{k=0}^{a_{SR}+a_1} (k-1)! \left(\frac{1-}{+\$}\right)^{k\#} : \quad (17)$$

The CDF of Z_1 is calculated as:

$$F_{Z_1}(x) = \Pr\left[\min\left(\frac{x_1}{R}; \frac{x_1}{RU_1}\right) < x\right] = 1 - \underbrace{\Pr\left(\frac{x_1}{R} > x\right)}_{A_1} \underbrace{\Pr\left(\frac{x_1}{RU_1} > x\right)}_{A_2} \quad (18)$$

With the help of (4), the term A_1 is formulate by:

$$A_1 = \Pr\left[\left|\hat{h}_{SR}\right|^2 > \frac{x\left(d_{SR}\sigma_{SR}^2 + 1\right)}{d_{SR} - x\, d_{SR}(1-)}\right] = \int_{\frac{x\left(d_{SR}\sigma_{SR}^2+1\right)}{d_{SR}-x\,d_{SR}(1-)}}^{\infty} f_{\left|\hat{h}_{SR}\right|^2}(x)\,dx \quad (19)$$

Putting (9) into (19), (19) is rewrite as:

$$A_1 = \frac{(K_{SR}+1)e^{-K_{SR}}}{SR} \int_{\frac{x\left(d_{SR}\sigma_{SR}^2+1\right)}{d_{SR}-x\,d_{SR}(1-)}}^{\infty} e^{-\frac{(1+K_{SR})}{SR}x} I_0\left(2\sqrt{\frac{K_{SR}(1+K_{SR})x}{SR}}\right)dx \quad (20)$$

Based on [25], we can write A_1 as:

$$A_1 = \sum_{n_{SR}=0}^{n_{SR}} \frac{K_{SR}^{n_{SR}} e^{-K_{SR}}}{(n_{SR}!)^2} \left(\frac{1+K_{SR}}{SR}\right)^{n_{SR}+1} \int_{\frac{x\left(d_{SR}\sigma_{SR}^2+1\right)}{d_{SR}-x\,d_{SR}(1-)}}^{\infty} y^{n_{SR}} e^{-\frac{(1+K_{SR})}{K_{SR}}y} dy \quad (21)$$

Moreover, with result in [25] A_1 can be obtained as:

$$A_1 = \sum_{n_{SR}=0}^{n_{SR}} \sum_{a_{SR}=0}^{a_{SR}} \frac{K_{SR}^{n_{SR}} e^{-K_{SR}}}{a_{SR}! n_{SR}!} \left(\frac{x}{-x(1-)}\right)^{a_{SR}} e^{-\frac{x}{x(1-)}x}; \quad (22)$$

where $= \frac{(1+K_{SR})\left(d_{SR}\sigma_{SR}^2+1\right)}{SR\ d_{SR}}$. Then, the second term A_2 of (18) is rewritten as:

$$A_2 = \Pr\left[\left|\hat{h}_{RU_1}\right|^2 > \frac{x\left(d_{RU_1}\sigma_1^2+1\right)}{d_{RU_1} - x\, d_{RU_1}(1-)}\right] = \int_{\frac{x\left(d_{RU_1}\sigma_1^2+1\right)}{d_{RU_1}-x\,d_{RU_1}(1-)}}^{\infty} f_{\left|\hat{h}_{RU_1}\right|^2}(x)\,dx: \quad (23)$$

Similarly, we can obtain A_2 as:

$$A_2 = \sum_{n_1=0}^{n_1} \sum_{a_1=0}^{a_1} \frac{K_{RU_1}^{n_1} e^{-K_{RU_1}}}{a_1! n_1!} \left(\frac{\#x}{-x(1-)}\right)^{a_1} e^{-\frac{\#x}{x(1-)}}; \quad (24)$$

where $\# = \frac{\left(1+K_{RU_1}\right)\left(d_{RU_1}\sigma_{RU_1}^2+1\right)}{RU_1\ d_{RU_1}}$.

Putting (22) and (24) into (18), we complete the proof.

4. NUMERICAL RESULTS

In this section, we set = 0:85, $\sim^2 = \sim^2_{SR} = \sim^2_{RU_1} = \sim^2_{RU_2}$ $K = K_{SR} = K_{RU_1} = K_{RU_1} = 2$, $_{SR} = _{RU_1} = _{RU_2} = 1$, = 2, $d_{SR} = 5m$, $d_{RD_1} = 10m$ and $d_{RD_2} = 5m$. We conduct 10^6 times for Monte-Carlo simulation. As can be seen in Figure 2, ergodic capacity increases significantly when value of SNR goes from 20 dB to 50 dB. Due to different power allocation factors and decoding procedure, two users show performance gap of ergodic capacity, i.e. at range SNR from 0 to 35 dB, performance of two users is similar, bigger gap among two users exist when SNR is greater than 35 dB. It is intuitively that Monte-Carlo simulation and analytical results are same, which shows the exactness of derivations.

We can see the impact of CSI imperfect levels on the ergodic performance, shown in Figure 3. At higher SNR region, SINR to detect signal at destination can be improved, then ergodic capacity is better as well. In this figure, $\sim^2$ = 0:01 is reported as best case for both users.

In Figure 4, the performance gap among two users depends on power allocation factor . Therefore, by adjusting such factor , the gap will be changed. Since NOMA benefits to the fairness, this modification of factor will satisfy the users' demand properly. In Figure 5, the quality of channel decide the height of curves of ergodic capacity. In this circumstance, K = 5 is reported as the best etgodic performance for three considered cases.

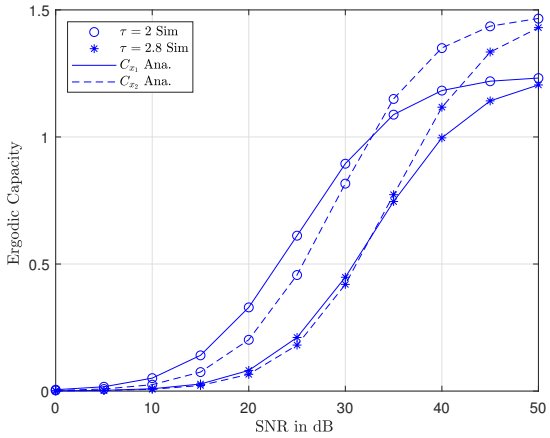

Figure 2. Ergodic capacity vs signal to noise ratio (SNR) in dB with different

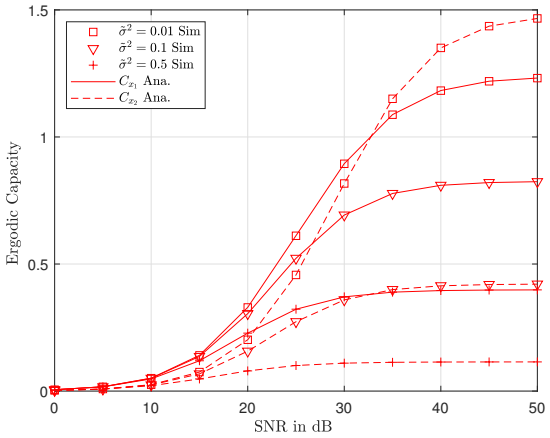

Figure 3. Ergodic capacity vs signal to noise ratio (SNR) in dB with different $\sim^2$

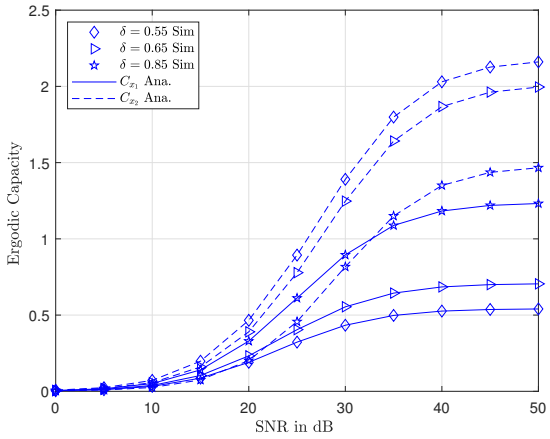

Figure 4. Ergodic capacity vs signal to noise ratio (SNR) in dB with different

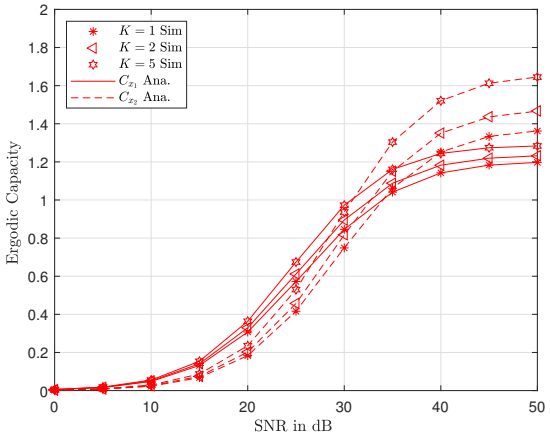

Figure 5. Ergodic capacity vs signal to noise ratio (SNR) with different K

5. CONCLUSION

This paper has explored the impact of CSI imperfection on the ergodic capacity of a two-user cooperative NOMA network. We conduct Rician fading model for wireless transmission from the source to destination with the assistance of relay. The fixed power allocation factor scheme is adopted and SIC is useful to detect signals at destinations. We derived the closed-form expression of ergodic capacity and verify all main system parameters to how they make influence on the system performance. In future work, we deploy multiple destinations to highlight how interference among many users in a group of destinations which get benefit from NOMA.

REFERENCES

[1] G. Li and D. Mishra, "Cooperative NOMA networks: User cooperation or relay cooperation?," in *ICC 2020-2020 IEEE International Conference on Communications (ICC)*, 2020, pp. 1-6, doi: 10.1109/ICC40277.2020.9148973.

[2] L. Dai, B. Wang, Y. Yuan, S. Han, C. I, and Z. Wang, "Non-orthogonal multiple access for 5G: Solutions, challenges, opportunities, and future research trends," in *IEEE Communications Magazine*, vol. 53, no. 9, pp. 74–81, Sep. 2015, doi: 10.1109/MCOM.2015.7263349.

[3] Y. Liu, Z. Qin, M. Elkashlan, Z. Ding, A. Nallanathan, and L. Hanzo, "Nonorthogonal multiple access for 5G and beyond," *Proc. IEEE.*, vol. 105, no. 12, pp. 2347–2381, Dec. 2017.

[4] J. N. Laneman, D. N. C. Tse, and G. W. Wornell, "Cooperative diversity in wireless networks: efficient protocols and outage behavior," *IEEE Transactions on Information theory*, vol. 50, no. 12, pp. 3062–3080, December 2004, doi: 10.1109/TIT.2004.838089.

[5] Dinh-Thuan Do, Tu-Trinh Nguyen Nguyen, Chi-Bao Le, M. Voznak, Z. Kaleem, and K. M. Rabie, "UAV Relaying Enabled NOMA Network with Hybrid Duplexing and Multiple Antennas," *IEEE Access*, vol. 8, pp. 186993-187007, 2020, doi: 10.1109/ACCESS.2020.3030221.

[6] J. Men and J. Ge, "Non-orthogonal multiple access for multiple-antenna relaying networks," *IEEE Commun. Lett.*, vol. 19, no. 10, pp. 1686–1689, Oct. 2015, doi: 10.1109/LCOMM.2015.2472006.

[7] Dinh-Thuan Do, M. -S. Van Nguyen, M. Voznak, A. Kwasinski, and J. N. de Souza, "Performance Analysis of Clustering Car-Following V2X System with Wireless Power Transfer and Massive Connections," in *IEEE Internet of Things Journal*, 2021, doi: 10.1109/JIOT.2021.3070744.

[8] Dinh-Thuan Do, M. -S. Van Nguyen, T.-A. Hoang, and B. M. Lee, "Exploiting Joint Base Station Equipped Multiple Antenna and Full-Duplex D2D Users in Power Domain Division Based Multiple Access Networks," *Sensors*, vol. 19, no. 11, p. 2475, 2019, doi: 10.3390/s19112475.

[9] Dinh-Thuan Do, A. Le, and B. M. Lee, "NOMA in Cooperative Underlay Cognitive Radio Networks Under Imperfect SIC," *IEEE Access*, vol. 8, pp. 86180-86195, 2020, doi: 10.1109/ACCESS.2020.2992660.

[10] G. Li, D. Mishra, and H. Jiang, "Cooperative NOMA with incremental relaying: Performance analysis and optimization," *IEEE Transactions on Vehicular Technology*, vol. 67, no. 11, pp. 11291-11295, November 2018, doi: 10.1109/TVT.2018.2869531.

[11] Z. Ding, H. Dai, and H. V. Poor, "Relay selection for cooperative NOMA," *IEEE Wireless Commun. Lett.*, vol. 5, no. 4, pp. 416–419, Aug. 2016, doi: 10.1109/LWC.2016.2574709.

[12] Z. Yang, Z. Ding, Y. Wu, and P. Fan, "Novel relay selection strategies for cooperative NOMA," *IEEE Trans. Veh. Technol.*, vol. 66, no. 11, pp. 10 114–10 123, Nov. 2017, doi: 10.1109/TVT.2017.2752264.

[13] Z. Ding, M. Peng, and H. V. Poor, "Cooperative non-orthogonal multiple access in 5G systems," *IEEE Commun. Lett.*, vol. 19, no. 8, pp. 1462–1465, Aug. 2015, doi: 10.1109/LCOMM.2015.2441064.

[14] X. Liu, H. Ding and S. Hu, "Uplink Resource Allocation for NOMA-based Hybrid Spectrum Access in 6G-enabled Cognitive Internet of Things," in *IEEE Internet of Things Journal*, 2020, doi: 10.1109/JIOT.2020.3007017.

[15] Z. Na, Y. Liu, J. Shi, C. Liu, and Z. Gao, "UAV-supported Clustered NOMA for 6G-enabled Internet of Things: Trajectory Planning and Resource Allocation," in *IEEE Internet of Things Journal*, 2020, doi: 10.1109/JIOT.2020.3004432.

[16] J.-B. Kim and I.-H. Lee, "Non-orthogonal multiple access in coordinated direct and relay transmission," *IEEE Commun. Lett.*, vol. 19, no. 11, pp. 2037–2040, Nov. 2015, doi: 10.1109/LCOMM.2015.2474856.

[17] X. Li et al., "Cooperative wireless-powered NOMA relaying for B5G IoT networks with hardware impairments and channel estimation errors," *IEEE Internet of Things Journal*, vol. 8, no. 7, pp. 5453-5467, 1 April1, 2021, doi: 10.1109/JIOT.2020.3029754.

[18] X. Yue, Y. Liu, S. Kang, and A. Nallanathan, "Performance analysis of NOMA with fixed gain relaying over Nakagami-m fading channels," *IEEE Access*, vol. 5, pp. 5445–5454, 2017, doi: 10.1109/ACCESS.2017.2677504.

[19] H. Sun, Q. Wang, R. Q. Hu, and Y. Qian, "Outage probability study in a NOMA relay system," in *2017 IEEE Wireless Communications and Networking Conference (WCNC)*, San Francisco, CA, USA, March 2017, pp. 1–6, doi: 10.1109/WCNC.2017.7925775.

[20] M. F. Kader, M. B. Shahab, and S. Y. Shin, "Exploiting non-orthogonal multiple access in cooperative relay sharing," *IEEE Commun. Lett.*, vol. 21, no. 5, pp. 1159–1162, May 2017, doi: 10.1109/LCOMM.2017.2653777.

[21] X. Liang, Y. Wu, D. W. K. Ng, Y. Zuo, S. Jin, and H. Zhu, "Outage performance for cooperative NOMA transmission with an AF relay," *IEEE Communications Letters*, vol. 21, no. 11, pp. 2428–2431, November 2017, doi: 10.1109/LCOMM.2017.2681661.

[22] R. Jiao, L. Dai, J. Zhang, R. MacKenzie and M. Hao, "On the Performance of NOMA-Based Cooperative Relaying Systems Over Rician Fading Channels," *IEEE Transactions on Vehicular Technology*, vol. 66, no. 12, pp. 11409-11413, Dec. 2017, doi: 10.1109/TVT.2017.2728608.

[23] Dinh-Thuan Do and Anh-Tu Le, "NOMA based cognitive relaying: Transceiver hardware impairments, relay selection policies and outage performance comparison," *Computer Communications*, vol. 146, pp. 144–154, July 2019, doi: 10.1016/j.comcom.2019.07.023.

[24] C. Deng, M. Liu, X. Li and Y. Liu, "Hardware Impairments Aware Full-Duplex NOMA Networks Over Rician Fading Channels," *IEEE Systems Journal*, vol. 15, no. 2, pp. 2515–2518, 2020, doi: 10.1109/JSYST.2020.2984641.

[25] I. S. Gradshteyn and I. M. Ryzhik, *Table of Integrals, Series and Products*, 6th ed. New York, NY, USA: Academic Press, 2000.